# Hepatobiliary Imaging Update

**Maggie Chester and Jerry Glowniak**

*Veterans Affairs Medical Center and Oregon Health Sciences University, Portland, Oregon*

***This is the first article in a four-part series on interventional nuclear medicine. Upon completion, the nuclear medicine technologist should be able to (1) list the advantages of using interventional hepatic imaging, (2) identify the benefit in calculating HEF, and (3) utilize the HEF calculation method when appropriate.***

Scintigraphic assessment of hepatobiliary function began in the 1950s with the introduction of iodine-131 ($^{131}$I) Rose bengal (*1*). Due to the poor imaging characteristics of $^{131}$I, numerous attempts were made to find a technetium-99m ($^{99m}$Tc) labeled hepatobiliary agent (*2*). The most useful of the several $^{99m}$Tc-labeled agents that were investigated were the iminodiacetic acid (IDA) analogs, which were introduced in the mid 1970s (*3*).

The IDA analogs are derivatives of lidocaine. By placing different substituents on the phenyl ring, various IDA analogs are produced which have different biological characteristics (Fig. 1). In general, the more lipophilic substitutions produce IDA agents that have faster hepatic uptakes and can be used with greater degrees of hepatic dysfunction. At present, there are two IDA agents approved by the Food and Drug Administration (FDA): diisopropyl IDA (DISIDA, disofenin) (Hepatolite®, Du Pont Radiopharmaceuticals, N. Billerica, MA) and m-bromotrimethyl IDA (TMBIDA, mebrofenin) (Choletec®, Squibb Diagnostics, New Brunswick, NJ). Mebrofenin has a slightly faster hepatic uptake and excretion than disofenin and is becoming more widely used since it received FDA approval in 1987.

The most widespread use of hepatobiliary imaging is for the evaluation of acute cholecystitis. Sensitivities and specificities of greater than 94% have been documented in several large imaging series (*4*). More recently, quantitative measures of liver and gallbladder function have been introduced. In a previous continuing education article in this journal (*5*), methods of quantifying hepatobiliary function were described, which included calculating the half-time of liver excretion and the gallbladder ejection fraction (EF) after the injection of cholecystokinin (CCK) (Kinevac®, Squibb Diagnostics, New Brunswick, NJ). A brief description of the hepatic extraction fraction (HEF) was given; the technique used quantifies hepatocyte function more accurately than does excretion half-time. Since publication of the previous article (*5*), the HEF has become more widely used as a measure of hepatocyte function, and nearly all the major nuclear medicine software vendors include programs for calculating the HEF.

In this article, we will describe new observations and methods used in hepatobiliary imaging. The following topics will be discussed: (1) the use of morphine as an aid in the diagnosis of acute cholecystitis, (2) the rim sign in the diagnosis of acute cholecystitis, and (3) methods for calculating the HEF.

## MORPHINE-AUGMENTED CHOLESCINTIGRAPHY

In acute cholecystitis, the cystic duct becomes obstructed either by a gallbladder stone or by edema from the inflamed gallbladder (see Fig. 2). Acute cholecystitis is diagnosed when the gallbladder fails to visualize, and tracer is seen in the common bile duct or intestine. If tracer cannot reach the cystic duct, due to total obstruction of the common hepatic duct, then a HIDA study cannot be used to diagnose acute cholecystitis. Visualization of the gallbladder is an extremely reliable method for excluding acute cholecystitis. Results from several large imaging series indicate that gallbladder visualization rules out acute cholecystitis with a reliability (a negative predictive value) of 98% to 100% (*6*). Unfortunately, there are several circumstances in which nonvisualization of the gallbladder occurs when acute cholecystitis is not present, thus, the specificity of the test decreases (a lower positive predictive value).

Prolonged fasting (*7*), total parenteral nutrition (*8*), severe intercurrent illness (*9*), or chronic cholecystitis (*10*) can cause delayed visualization or nonvisualization of the gallbladder. This occurs because bile completely fills the gallbladder when the gallbladder is not stimulated to contract for long periods, as in fasting, or when gallbladder contraction by endogenous CCK is reduced as in chronic cholecystitis. Thus, the completely filled gallbladder cannot accept the radiolabeled bile. Specificity can be improved by delayed imaging (*11*) or pretreatment with CCK. These methods have their draw-

For reprints contact: Maggie Chester, VA Medical Center (115), PO Box 1034, Portland, Oregon 97207.

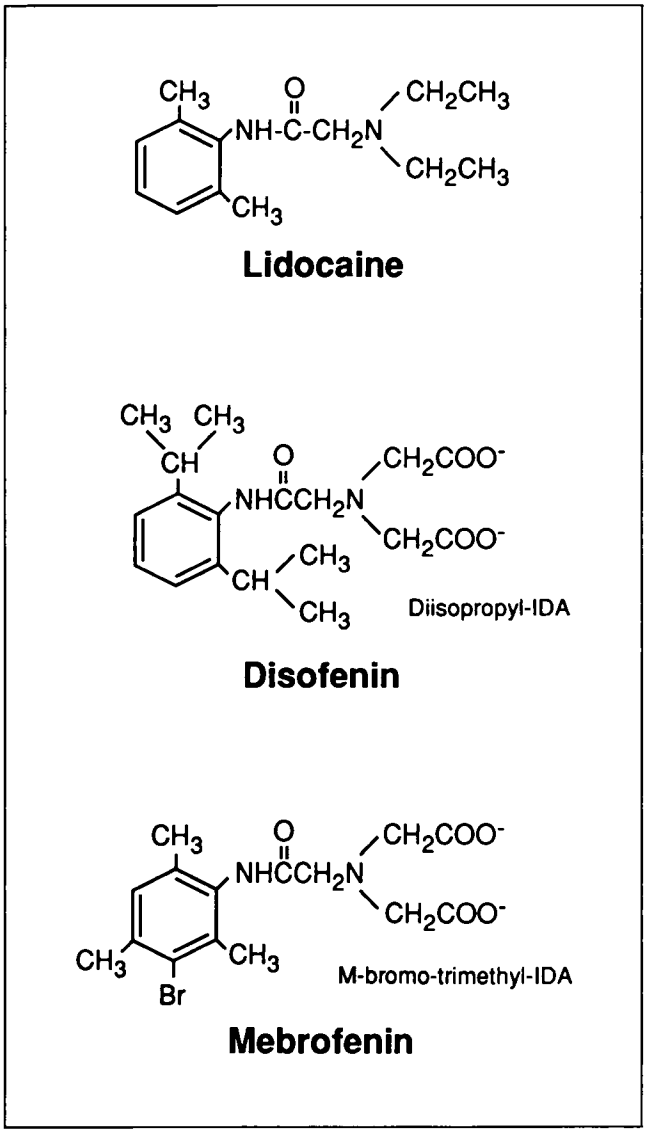


**FIG. 1.** Lidocaine (top figure) is the parent compound from which all IDA agents are derived. The two FDA approved IDA analogs are disofenin and mebrofenin.

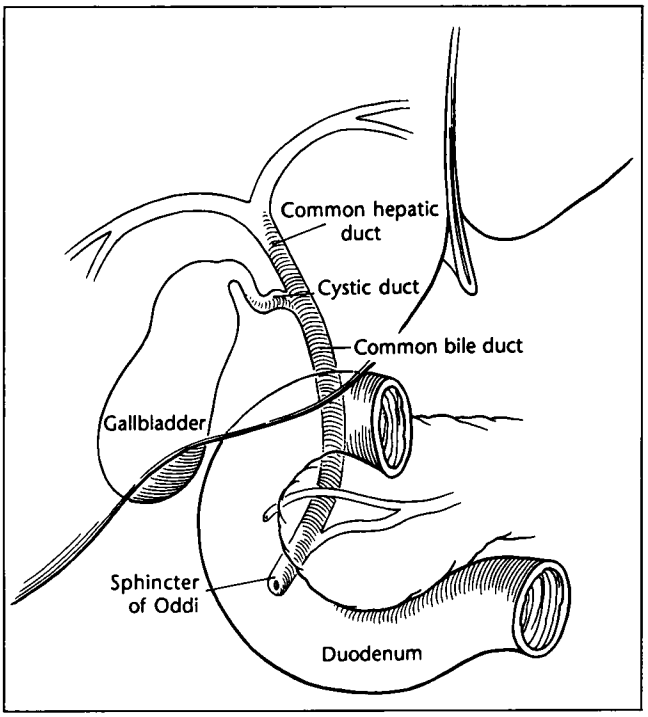


**FIG. 2.** Anatomy of hepatobiliary system. Common hepatic duct joins cystic duct to form common bile duct. Sphincter of Oddi is muscular band at termination of common bile duct that controls bile flow into duodenum.

backs, however. Both methods increase the length of the study. If tracer is cleared rapidly from the liver, delayed imaging may be useless if there is little or no tracer in the liver after 1 hr of imaging.

In the last several years, intravenous (IV) morphine has been used to hasten gallbladder visualization in hepatobiliary studies. Bile flows from the common bile duct through the sphincter of Oddi into the duodenum (Fig. 2). Morphine causes constriction of the sphincter of Oddi diverting bile flow from the duodenum into the gallbladder if the cystic duct is patent. Several studies have shown that this technique can speed gallbladder visualization, improving specificity (fewer false positives), without losing sensitivity (*12–14*). If the gallbladder does not visualize by 60 min, most authors recommend giving 0.04 mg/kg IV morphine over 3 min and imaging for an additional 30 min (*2,15*). If the gallbladder does not visualize within 30 min after morphine injection, the study is terminated and interpreted as showing acute cholecystitis.

Figure 3 demonstrates nonvisualization of a patient's gallbladder at 1 hr. The patient was then injected with morphine, and the gallbladder was clearly visualized 30 min after the injection.

Several pitfalls should be kept in mind when using morphine. Morphine should not be given until activity is seen in the common bile duct or intestines, since radioactive bile must be present at the cystic duct for visualization of the gallbladder to occur. Similarly, since tracer can be excreted rapidly from a normal liver, there must be tracer left in the liver at the time of morphine injection so that radioactive bile can flow into the gallbladder. If there is too little tracer left in the liver at 60 min for an adequate study, a second dose of tracer may be given and morphine injected when the common bile duct is visualized. Alternatively, morphine can be given before 60 min if the common bile duct is well visualized. If morphine is given and the gallbladder visualizes, and then CCK is injected, the gallbladder EF cannot be measured. CCK may not be able to relax the sphincter of Oddi after morphine injection, resulting in falsely low values for the EF.

## THE RIM SIGN

Patients with acute cholecystitis can usually be treated conservatively with bed rest, restriction of oral intake, and analgesics as needed for pain. Inflammation and cystic duct obstruction will subside over several days. In some instances,

however, inflammation may be so severe that the blood supply to the gallbladder is interrupted, resulting in gallbladder necrosis and gangrene. Patients with these conditions must be taken to surgery as soon as possible to prevent abscess formation, peritonitis, or sepsis.

Several reports have shown that patients with a gangrenous gallbladder have increased tracer uptake and slow tracer clearance from the liver parenchyma adjacent to the gallbladder (*16–18*) (Fig. 4). The mechanism that is most likely responsible for this pattern is the inflammatory response spreading to the adjacent liver. Increased blood flow causes greater tracer delivery. The inflammation, however, either impedes bile excretion by the hepatocyte and/or blocks biliary radicles by edema, causing persistence of tracer activity at later times. Since this activity forms an outline of the gallbladder fossa in the liver, the term "rim sign" has been used for this pattern. When the rim sign is seen with nonvisualization of the gallbladder, the referring physicians should be informed that a gangrenous gallbladder may be present.

One report (*18*) further documents the usefulness of flow studies in conjunction with a HIDA study to diagnose gangrenous cholecystitis. In this report, 88% of patients with gangrenous cholecystitis had a positive flow study, while only 46% had a rim sign.

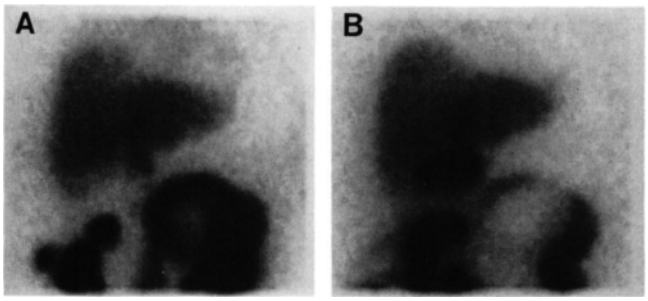


**FIG. 3.** Gallbladder has not visualized 60 min after injection of tracer. IV morphine was given and imaging continued for 30 min. (A) At 4 min after morphine injection no tracer is seen in gallbladder fossa. (B) By 30 min, gallbladder is clearly seen.

## THE HEPATIC EXTRACTION FRACTION

The EF of a tracer by an organ is defined as the percent or fraction of the tracer removed by the organ after a single pass of the tracer through the organ. For example, the cardiac EF for thallium is 88% (*19*). The most direct way to measure the HEF would be to inject a known quantity of tracer directly into the blood supply of the liver (the hepatic artery and portal vein) and measure the amount of tracer taken up in the first pass through the liver. The HEF for IDA agents has been measured directly and found to be greater than 95% in an intact liver (*20*). Furthermore, liver injury by ischemia causes a fall in the HEF (*21*) suggesting that the HEF is a direct measure of hepatocyte integrity.

Unfortunately, it is not possible to directly measure the HEF after peripheral IV tracer injection since only a fraction of the bolus goes directly to the liver and as time passes, tracer is simultaneously removed from the blood and excreted into the bile. Thus, time-activity curves (TACs) of the liver and parameters derived from it such as the excretion half-time, represent both hepatocyte uptake and biliary excretion. TACs are relatively nonspecific and may have a similar appearance with different disease processes. For example, in acute, total obstruction of the common duct, the excretion half-time will be prolonged because of stasis of bile flow even though hepatocyte function is intact. In cirrhosis, tracer uptake is prolonged because of hepatocyte injury, and this in turn prolongs the excretion half-time.

In order to measure hepatocyte function independently from the measurement of biliary abnormalities, an indirect

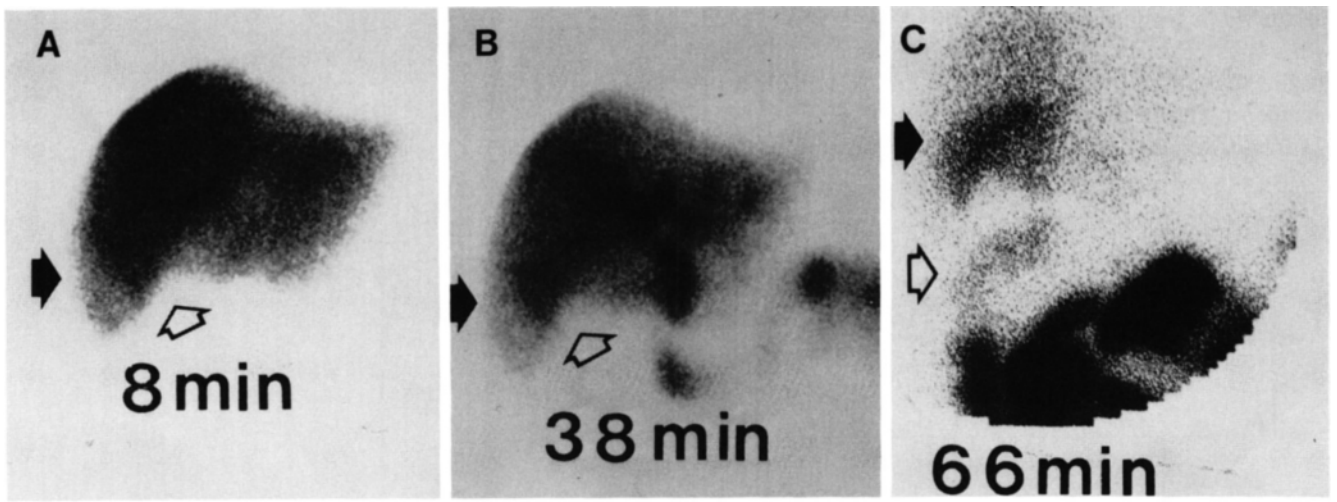


**FIG. 4.** (A) 8 min after tracer injection, no tracer is seen in gallbladder fossa (open arrow), but there is a clear difference in hepatic uptake in right lower lobe (solid arrow). (B) At 38 min, no tracer is seen in gallbladder fossa, but is well seen in common bile duct. Activity in right lower lobe appears unchanged while diminishing in adjacent liver. (C) At 66 min, activity in liver surrounding gallbladder fossa (solid arrow) is much greater than activity in rest of liver (the rim sign). Open arrow shows intestinal activity, but no activity is seen in gallbladder fossa. Patient had gangrenous gallbladder at surgery.

method has been developed to measure the HEF by using deconvolutional analysis (*20–22*). In this technique a region of interest (ROI) is placed over the heart. A TAC (the input function) is generated which represents the concentration of tracer in the blood that is being presented to the liver. The heart ROI is not used for background subtraction. A second ROI is placed over the hepatic parenchyma to obtain a second TAC (the response function). At any given time, the activity within a region of the liver is the net result of the total amount of tracer taken up by the hepatocytes minus the total excreted.

Deconvolutional analysis corrects the hepatic TAC for the prolonged period of tracer uptake from the blood and for the continuously decreasing concentration of tracer in the blood. The result of the analysis is a curve (the deconvoluted hepatic TAC) which defines the hepatic retention function. This function is the hepatic TAC that would result from a bolus injection of all the tracer into the hepatic artery and portal vein and measurement of the tracer that exits the liver and is removed from the circulation and biliary tree (*22*).

Figure 5 shows two hypothetical hepatic retention functions, one for a normal liver (Fig. 5A) and one for a patient with severe hepatocellular disease (Fig. 5B). Initially, all the tracer from the bolus injection is within the liver and the curve attains its maximum value, which is then set as equal to 100%. Tracer which is not taken up by the hepatocytes rapidly exits the liver in the venous blood. This initial phase has been termed the vascular phase (*22*).

The later portion of the curve is termed the hepatocyte retention phase and represents hepatic excretion of the initial tracer uptake. A monoexponential curve is fitted through the data points after the vascular phase and extrapolated to the peak of the vascular curve. Dividing the extrapolated value by the peak value during the vascular phase gives the fraction of the bolus that was taken up by the hepatocytes, the HEF.

To measure an HEF, a standard hepatobiliary study is performed. The heart is included in the field of view. Acquisition is started at least 1 min before tracer injection, and data is acquired in 1-min frames. A 64 x 64 x 16 matrix is used with a large field of view (LFOV) gamma camera. Although imaging is continued for 1 hr, only the first 30 to 32 min of data (depending on the program) are used.

A frame from the beginning of the study is selected in which the liver and heart are well seen for placement of the heart and liver ROIs (Fig. 6). It is important that no biliary activity (gallbladder or major bile ducts) or vascular activity (right kidney, aorta, inferior vena cava) is included in the hepatic ROI. Including these structures in the hepatic ROI may artifactually lower the HEF. More than one liver ROI can be drawn to measure the HEF in different parts of liver. All ROIs must stay below the superior margin of the liver, especially in the left lobe since activity from the heart may scatter into a left lobe ROI. After drawing the ROIs, it is a good idea to view the first 30 min of the study in cine mode with the ROIs to ensure that no biliary or vascular structures are in the hepatic ROIs and to check for patient motion. The heart ROI should correspond to the left ventricle.

After placement of the ROIs, our system (ADAC Laboratories, Milpitas, CA) will automatically calculate and display the deconvolved data points and draw a fitted exponential curve utilizing the data points after the vascular phase. The Y-axis is scaled to 100% using the peak activity of the deconvolved liver TAC. The time at which this occurs is set equal to zero. The point where the fitted curve intersects the Y-axis is the HEF (Fig. 7).

The HEF is a useful method for evaluating patients with jaundice or abnormal liver function tests. The most important question when diagnosing such a patient is whether the abnormalities are due to intrinsic hepatic disease (e.g., cirrhosis or hepatitis) or are secondary to obstruction of the biliary tree (e.g., a stone in the common duct). In the former case, the HEF would be expected to be low and in the latter, normal, if obstruction has not been present for too long (prolonged obstruction will cause damage to the hepatocytes and a low HEF).

In one study (*22*), 32 patients with normal livers who had HIDA scans for acute cholecystitis had an average HEF of 99% with a lower limit of normal of 91% (mean−2 s.d.). Ten

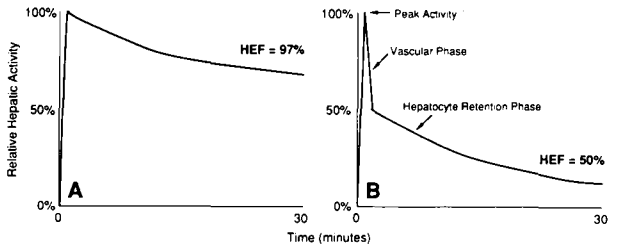


**FIG. 5.** Hypothetical deconvoluted liver time-activity curves in (A) normal liver and (B) cirrhotic liver. In both cases, initial vascular peak is seen and set equal to 100%. Peak is equivalent to bolus tracer injection into the hepatic blood supply. Fall after peak represents tracer not taken up in first pass. Extrapolating curve for hepatic retention phase back to vascular peak gives HEF. Adapted from (*22*).

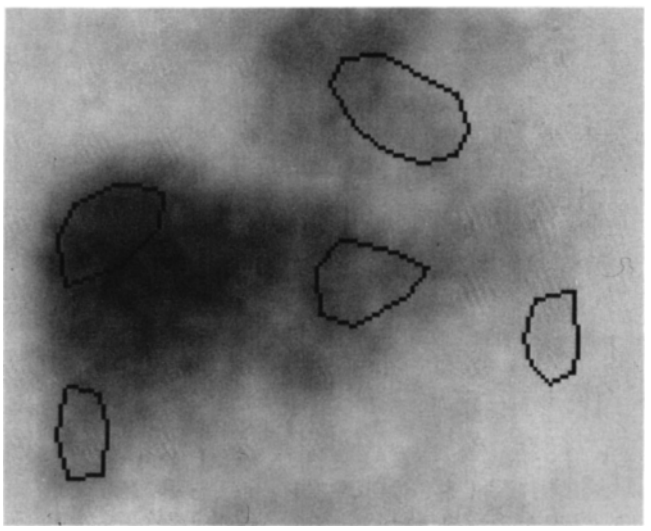

**FIG. 6.** Placement of ROIs in liver for measurement of regional HEFs. Heart ROI is used to measure the input function. Spleen ROI is required by software program to calculate hepatic excretion half-time but is not used in the calculation of HEF.

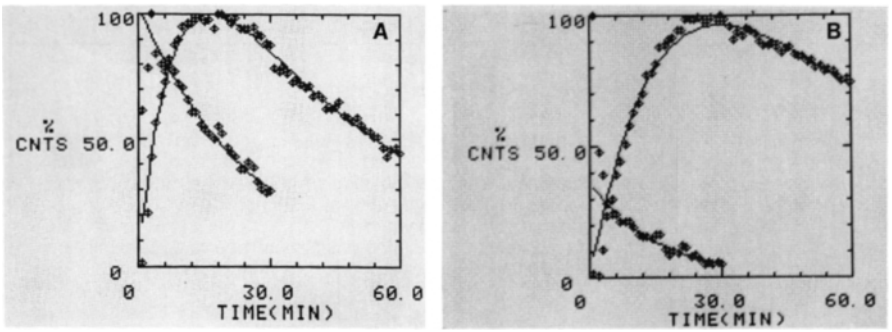


**FIG. 7.** Display of fitted hepatic time-activity curves (upper curves ending at 60 min) and deconvolved hepatic time-activity curves (lower curves ending at 30 min) for (A) normal liver and (B) patient with cirrhosis, using a commercial software program. HEF is where fitted deconvolved curve intersects Y-axis. HEF = 100% for normal liver and 37% in patient with cirrhosis.

patients with jaundice from acute biliary obstruction had an average HEF of 89% with a range of 64%–100%. The HEF was normal for the first two days in this group, but fell progressively to 65% by one week after the onset of obstruction. In 11 patients with hepatocyte dysfunction, the mean HEF was 41% with a range of 14%–77%.

The results suggest that the HEF can distinguish acute obstruction (less than one week) from hepatocellular disease. After one week, obstruction causes secondary hepatocyte dysfunction, and the HEF cannot reliably distinguish obstruction from hepatocyte injury. Nevertheless, the HEF can be used as a general method for following patients serially with liver disease and has been used to evaluate rejection in liver transplants.

## CONCLUSION

In summary, several new developments have occurred in hepatobiliary imaging that increase the diagnostic usefulness of the study. The use of morphine to hasten gallbladder visualization can reduce the time needed to diagnose acute cholecystitis. A positive radionuclide flow study and/or a rim sign in conjunction with nonvisualization of the gallbladder alerts the clinician to possible severe gallbladder inflammation and gangrene. The HEF is more specific than other quantitative measures of hepatic function and may allow the differentiation of extrahepatic biliary obstruction from hepatocyte injury. The HEF shows promise as a method for following patients with changing liver function and may be able to serve as a guide to therapy.

## REFERENCES


1. Taplin GV, Meredith OM Jr, Dade H. The radioactive (I-131 tagged) rose-bengal uptake excretion test for liver function using external gamma ray scintillation counting technique. *J Lab Clin Med* 1955;45:665–678.
2. Krishnamurthy GT, Turner FE. Pharmacokinetics and clinical application of technetium 99m-labeled hepatobiliary agents. *Semin Nucl Med* 1990;20:130–149.
3. Loberg MD, Cooper M, Harvey E, et al. Development of new radiopharmaceutical based on N-substitution of iminodiacetic acid. *J Nucl Med* 1976;17:633–638.
4. Weissmann HS, Freeman LM. The biliary tract. In: Freeman LM, ed. *Freeman and Johnson's Clinical Radionuclide Imaging.* Vol 2. 3rd ed. Orlando, FL: Grune & Stratton; 1984:879–1049.
5. Gilbert SA, Brown PH, Krishnamurthy GT. Quantitative nuclear hepatology. *J Nucl Med Technol* 1987;15:38–43.
6. Weissmann HS, Freeman LM. The biliary tract. In: Freeman LM, ed. *Freeman and Johnson's Clinical Radionuclide Imaging.* Vol 2. 3rd ed. Orlando, FL: Grune & Stratton; 1984:924.
7. Larsen MJ, Klingensmith WC, Kuni CC. Radionuclide hepatobiliary imaging: nonvisualization of the gallbladder secondary to prolonged fasting. *J Nucl Med* 1982;23:1003–1005.
8. Shuman WP, Gibbs P, Rudd TG. PIPIDA scintigraphy for cholecystitis: false positives in alcoholism and total parenteral nutrition. *Am J Roetengol* 1982;138:1–5.
9. Kalff V, Froelich JW, Lloyd R, Thrall JH. Predictive value of an abnormal hepatobiliary scan in patients with severe intercurrent illness. *Radiology* 1983;146:191–194.
10. Weissmann HS, Badia J, Sugarman LA, et al. Spectrum of 99m-Tc-IDA cholescintigraphic patterns in acute cholecystitis. *Radiology* 1981;138:167–175.
11. Freitas JE, Coleman RE. Nagle CE, Bree RL, Krewer KD, Gross MD. Influence of scan and pathologic criteria on the specificity of cholescintigraphy: concise communication. *J Nucl Med* 1983;24:876–879.
12. Choy D, Shi EC, McLean RG, Hoschl R, Murray IPC, Ham JM. Cholescintigraphy in acute cholecystitis: use of intravenous morphine. *Radiology* 1984;151:203–207.
13. Vasquez TE, Rimkus DS, Pretorius HT, Greenspan G. Intravenous administration of morphine sulfate in hepatobiliary imaging for acute cholecystitis: a review of clinical efficacy. *Nucl Med Commun* 1988;9:217–222.
14. Fink-Bennett D, Balon H, Robbins T, Tsai D. Morphine-augmented cholescintigraphy: its efficacy in detecting acute cholecystitis. *J Nucl Med* 1991;32:1231–1233.
15. Fink-Bennett D. Augmented cholescintigraphy: its role in detecting acute and chronic disorders of the hepatobiliary tree. *Semin in Nucl Med* 1991;11:128–139.
16. Brachman MB, Tanasescu DE, Ramanna L, Waxman AD. Acute gangrenous cholecystitis: radionuclide diagnosis. *Radiology* 1984;151:209–211.
17. Meekin GK, Ziessman HA, Klappenbach RS. Prognostic value and pathophysiologic significance of the rim sign in cholescintigraphy. *J Nucl Med* 1987;28:1679–1682.
18. Colletti PM, Ralls PW, Siegel ME, Halls JM. Acute cholecystitis: diagnosis with radionuclide angiography. *Radiology* 1987;163:615–618.
19. Weich HF, Strauss HW, Pitt B. The extraction of thallium-201 by the myocardium. *Circulation* 1977;56:188–191.
20. Galli G, Orlando P, Massari P, et al. 99m-Tc-diethyl-IDA: the extraction efficiency of the liver. *Eur J Nucl Med* 1983;8:187–190.
21. Tagge E, Campbell DA Jr, Reichle R, et al. Quantitative scintigraphy with deconvolutional analysis for the dynamic measurement of hepatic function. *J Surg Res* 1987;42:605–612.
22. Juni JE, Reichle R. Measurement of hepatocellular function with deconvolutional analysis: application in the differential diagnosis of acute jaundice. *Radiology* 1990;177:171–175.